

Ion channeling in natural diamond. II. Critical angles

T. E. Derry, R. W. Fearick, and J. P. F. Sellschop

Nuclear Physics Research Unit, University of the Witwatersrand, Johannesburg, South Africa

(Received 10 August 1981; revised manuscript received 10 February 1982)

In this paper the critical angles for ions channeling in diamond single crystals are presented and considered. Careful attention was paid to experimental precautions to ensure reliable results. In diamond the thermal vibration amplitude is much less than the Thomas-Fermi screening distance even at ordinary temperatures, and this crystal can be expected to furnish a stringent test of theoretical critical-angle expressions which depend on the ratio of these two quantities. Data were taken for different axes and planes, for different ions and ion energies, and for different crystal temperatures. It is shown that most of the diamond data are in fact well represented by the established semiempirical expressions due to Barrett and can also be predicted accurately by the procedure of Varelas and Sizmann. This provides fresh confirmation of the continuum model for channeling and of some of the physical considerations underlying these theoretical approaches. The areas of disagreement serve to highlight important second-order effects of crystal geometry and can be understood within the terms of current theory.

I. INTRODUCTION

Reasons for the interest and importance of careful ion-channeling measurements on diamond have been outlined in a companion paper¹ (referred to henceforth as I) and illustrated by measurements of the minimum yield χ_{\min} of channeled ions which undergo Rutherford backscattering. Measurements of critical angles for channeling will be presented and considered in this contribution. Once again, diamond provides a test of prevailing theory under extreme conditions, and gives added insight into the physics of the channeling process.

II. EXPERIMENTAL

The experimental details for these measurements, including the sample selection and sample preparation procedures, together with other precautions, were the same as those described in I. Measurements were performed in the backscattering mode using protons with energies between 0.6 and 4.5 MeV and singly ionized helium ions with energies from 0.7 to 1.0 MeV. Several repetitions on different stones were made at room temperature, and a series of 1.0-MeV-proton measurements were made on one good stone up to 700 °C.

For each set of conditions, the critical angle $\psi_{1/2}$ (the half-width at half minimum of the dip obtained by plotting backscattered yield against incidence angle of the ions) was determined for the three most open axes of the diamond structure, viz., $\langle 110 \rangle$, $\langle 111 \rangle$, and $\langle 100 \rangle$, and for the three most open planes, viz., $\{110\}$, $\{111\}$, and $\{100\}$. A few measurements were

made for higher axes and planes. The goniometer precision was 0.01°, except for a few early measurements below 1.0 MeV, whose lower precision is reflected in the error bars on the relevant graphs. The channeling dips were plotted for a series of ion scattering depths z , enabling the extrapolation of $\psi_{1/2}$ to $z = 0$ (corresponding to zero dechanneling) for accurate comparison with theory.

Considerable attention was paid to the azimuthal orientation of the planes of the angular scans used in determining the axial critical angles. Work such as that of Barrett² has shown that numerous major and minor crystal planes may have a significant effect on the trajectories of ion beams in the region of a major

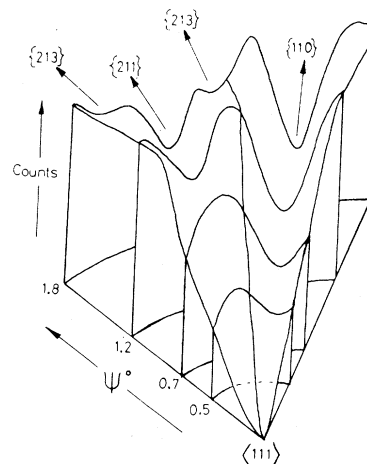


FIG. 1. Three-dimensional plot of conical scans about $\langle 111 \rangle$ (1.0-MeV protons; $\psi_{1/2} = 0.49^\circ$).

TABLE I. Optimum transaxial scan planes. Azimuthal angles are measured between the scan plane and a {110} crystal plane.

| Axis | Azimuth (deg) |
|-----------------------|---|
| $\langle 110 \rangle$ | 75 ± 5 |
| $\langle 111 \rangle$ | $17 \begin{smallmatrix} +1 \\ -2 \end{smallmatrix}$ |
| $\langle 100 \rangle$ | 30 ± 1 |

axis, and slightly different critical angles may result³ according to whether or not the scan lies along one of them. The effect was confirmed in diamond by making transaxial scans at different azimuths, and azimuthal ("conical") scans at different angular distances from the axis. A three-dimensional plot of such a conical scan for a $\langle 111 \rangle$ axis is represented in Fig. 1. It can be seen, and this is typical of other major axes, that, although only the lowest-index major planes are significant, their influence is felt over a large azimuthal range in the vicinity of the axis. In order to choose a scan plane with as little influence as possible from planar-channeling effects, the conical scans were examined and the azimuthal angle at which the yields rose to a maximum was noted (this happened at the same azimuth for each cone angle). This was equivalent to finding the azimuth for which the "narrowest" transaxial scan would be recorded. The chosen scan planes were adhered to for all the experiments; they should be valid for all diamond structure solids, and are listed in Table I. The permissible errors (chosen as the maximum deviation which made a negligible difference to the yield in the conical scans) are quite small if reproducible values of $\psi_{1/2}$ are to be determined.

Examination of the literature shows that many workers appear to ignore this problem. Some indeed have deliberately chosen to measure parallel to a major plane. This could be the source of some of the observed discrepancies with theory.

More widely recognized is the need to measure planar critical angles in a region free of the more close-packed axes lying in that plane; even fairly minor axes have a demonstrable effect.⁴ Both calculation and experiment were used to locate such axes in diamond and to avoid them.

III. RESULTS AND DISCUSSION

Examples of angular scans of the three major axes and three major planes for 1.0-MeV protons at room temperature are presented in Figs. 2(a) to 2(f), in the form of families of curves for different depths. They

are quite similar to those which have been reported for many other substances; an interesting feature thereof is considered towards the end of the paper. For planes, $\psi_{1/2}$ was independent of z to within the accuracy of the apparatus (0.01°); for axes, the depth dependence is depicted in Fig. 3. Different specimens differ slightly but the surface-extrapolated values of $\psi_{1/2}$ are the same to within 0.01° . There currently appears to be no analytic theory which gives the dependence of $\psi_{1/2}$ on z directly, but computer calculations based on a diffusion model, after the method of Kumakhov *et al.*,⁵ were able to reproduce the data quite well.

Similar channeling dips, depth dependences, and agreement between different specimens were obtained for other energies and for He^+ ions. At elevated temperatures the axial dips were narrower and shallower and the shoulders were reduced. These changes in the axial dips at elevated temperatures are shown in Figs. 4(a)–4(c).

The semiempirical expressions of Barrett⁶ have been found to provide the most accurate representation of the critical angles in different experiments on a wide variety of substances. They are, for axial channeling,

$$\psi_{1/2} = kF_{rs} \left(\frac{mu_1}{a} \right) \left[\frac{2Z_1 Z_2 e^2}{Ed} \right]^{1/2}, \quad (1)$$

and for planar channeling,

$$\psi_{1/2} = kF_{ps} \left(\frac{mu_1}{a}, \frac{d_p}{a} \right) \left[\frac{2\pi Z_1 Z_2 e^2 a N d_p}{E} \right]^{1/2}, \quad (2)$$

where Z_1 and Z_2 are the ion and target atomic numbers, respectively, e is the electron charge, E the ion energy, N the number of atoms per unit volume, d the row spacing, d_p the interplanar spacing, a the Thomas-Fermi screening distance of the ion-atom potential, and u_1 the rms thermal vibration amplitude in one dimension. The functions $F_{rs}(\xi)$ and $F_{ps}(\xi, \eta)$ may be found (tabulated or plotted) in Refs. 6 and 7, as may be the optimum values of the fitting parameters k and m . In the comparisons to be reported here, the values designated by Barrett as more appropriate for fitting the temperature dependence ($k = 0.83$ and $m = 1.2$ for axes, $k = 0.76$ and $m = 1.6$ for planes) were used also for fitting the ion and energy dependence, because they consistently gave a better fit. (Barrett's slightly different values for ion and energy dependence include an allowance for nonextrapolation to zero depth.) The values of u_1 were calculated using a Debye temperature of 1860 K ,⁸ and a was taken as $0.4685 Z_2^{-1/3} \text{ \AA}$.

In Fig. 5, the measured axial critical angles at room temperature are compared with those calculated from Eq. (1). The solid line at 45° represents perfect

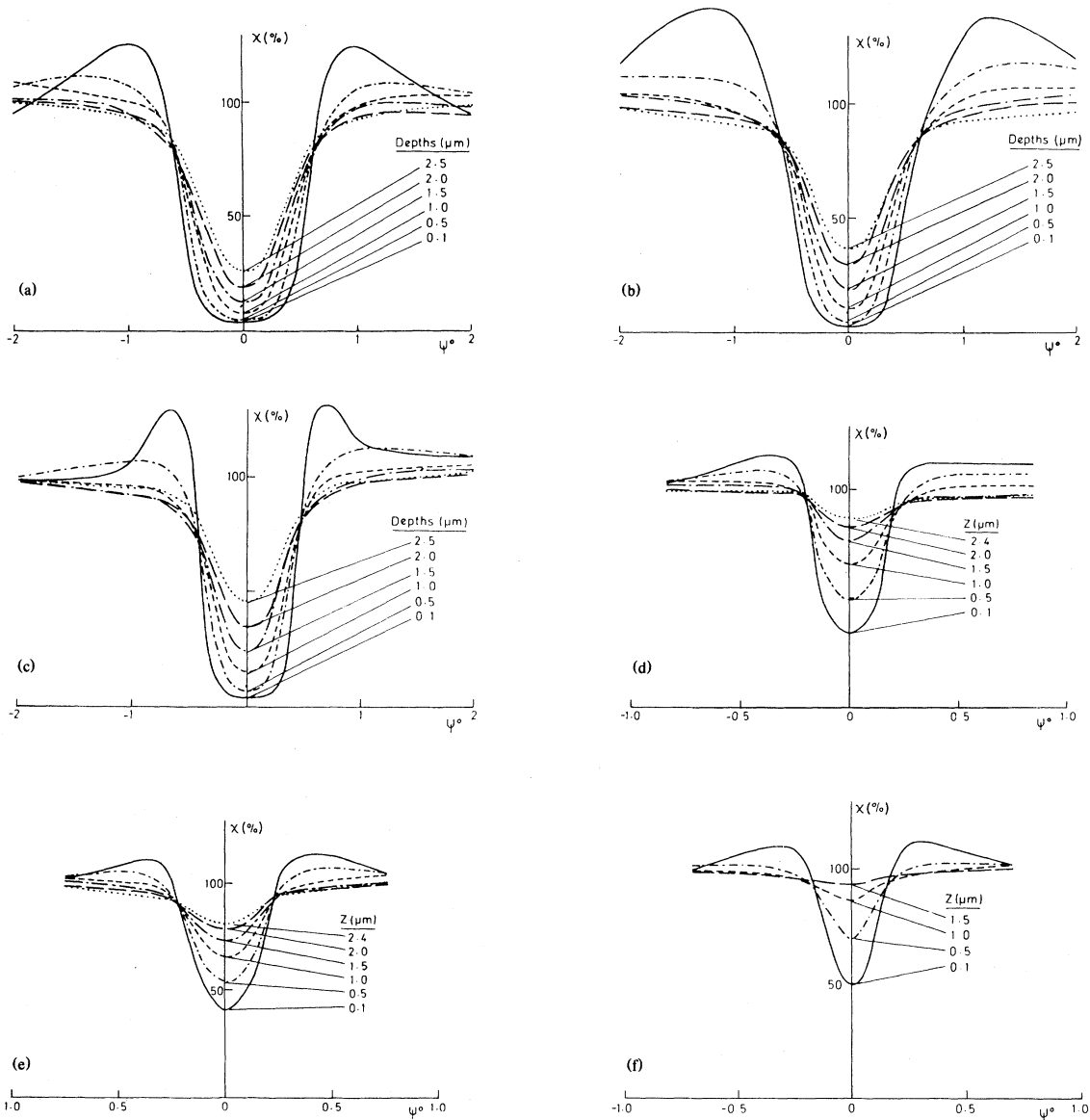


FIG. 2. 1.0-MeV-proton scans through axes and planes: (a), $\langle 110 \rangle$; (b), $\langle 111 \rangle$; (c), $\langle 100 \rangle$; (d), $\{110\}$; (e), $\{111\}$; (f), $\{100\}$.

agreement; the actual agreement is evidently very good indeed for the two most open axes ($\langle 110 \rangle$ and $\langle 111 \rangle$), except for the early data, below 1.0 MeV. The narrower axes consistently have smaller critical angles than predicted by Eq. (1). Most workers have tested this expression only for the one or two most open axes in each crystal, finding good agreement; it appears that for minor axes, a smaller value of k (about 0.76) is required. This is probably connected with the inter-row focusing effect observed by Barrett in his more recent Monte Carlo simulations,⁹ and to which he ascribes the deviation of k from 1.0. Since

this is an effect of detailed crystal geometry, different k 's are to be expected for different axes.

A comparison between measured planar critical angles and those predicted by Eq. (2) is made in Fig. 6. Once again, the agreement is very good, with the noticeable exception of the $\{111\}$ plane. Not only are the measured $\psi_{1/2}$ values high, but they equal or exceed those for the $\{110\}$ plane, although the $\{111\}$ has the smaller mean planar spacing.

The explanation is, however, readily apparent: the $\{111\}$ planes in the diamond structure have two sets of spacings, which were averaged to produce the

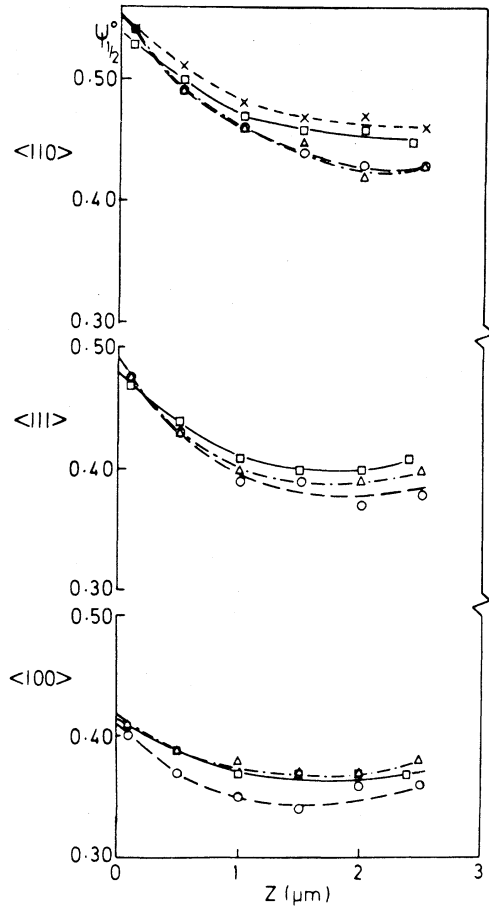


FIG. 3. Dependence of critical angle on depth for 1.0-MeV protons. Different symbols are for different diamond specimens.

value of d_p used in Eq. (2). However, these spacings are in the ratio 3:1, and presumably most ions will be channeled within the larger channel space. A rough calculation of the effective value of d_p in Eq. (2) gives 1.4 \AA , corresponding more closely to the larger of the two spacings (1.545 \AA) than to their mean (1.030 \AA).

A modified form of Eq. (2) was devised for unequally spaced planes by applying the continuum model^{10,11} in the light of the above consideration; the details are presented in an appendix to this paper. The new results agree well with the $\{111\}$ measurements. With some exceptions⁴ most workers have avoided the problem of unequally spaced (but homogeneous) planes by confining their measurements to other planes in each crystal. The present work shows that channeling between such planes admits of a simple description, at least when the spacings are very different.

The dependence of $\psi_{1/2}$ on u_1 is illustrated in Fig. 7 for temperatures from room temperature up to

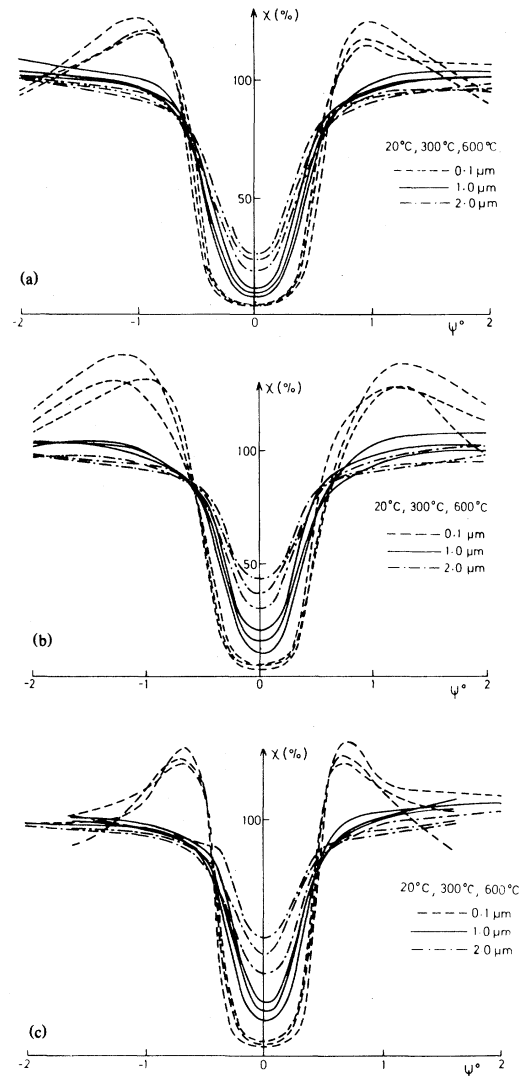


FIG. 4. Axial scans at different temperatures (1.0-MeV protons); narrowest dip at each depth is for highest temperature. (a), $\langle 110 \rangle$; (b), $\langle 111 \rangle$; (c), $\langle 100 \rangle$.

700°C , together with curves calculated from Eq. (1) (for axes) or Eq. (2) (for planes). The effect is very weak in the planar case, in keeping with experimental observations in other substances.⁴ Agreement between theory and experiment is quite good, with the exceptions already noted for the $\langle 100 \rangle$ axis and $\{111\}$ plane; an additional curve scaled to the room-temperature value is provided for $\langle 100 \rangle$. The error bars correspond to $\pm 0.01^\circ$, which is the error deduced both from the accuracy of the experiments themselves and from the reproducibility between different measurements.

It has been shown by Barrett⁶ that Eq. (1)

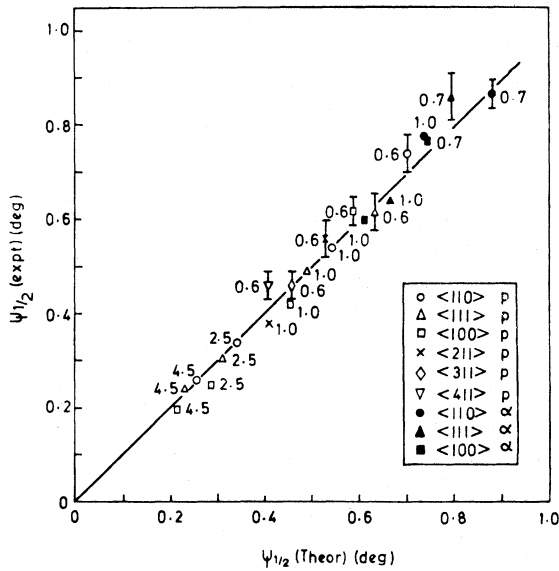


FIG. 5. Comparison of experimental values of $\psi_{1/2}$ for axes with theoretical values calculated from Eq. (1). Ion energies are indicated in MeV.

(although with $k = 1$ rather than 0.8) may be obtained by a purely analytic method¹² from the continuum model¹¹ when the ion-atom interaction is represented by the Molière potential. Thus a verification of this equation is largely a verification of the continuum model for channeling. Alternatively, both Eqs. (1) and (2) may be generated from the continu-

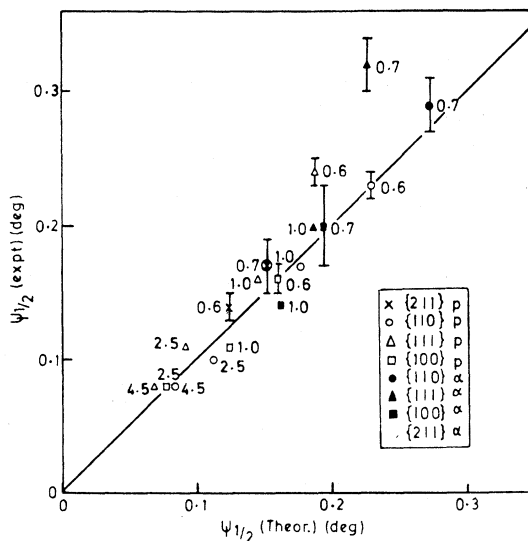


FIG. 6. Comparison of experimental values of $\psi_{1/2}$ for planes with theoretical values calculated from Eq. (2). Ion energies are indicated in MeV.

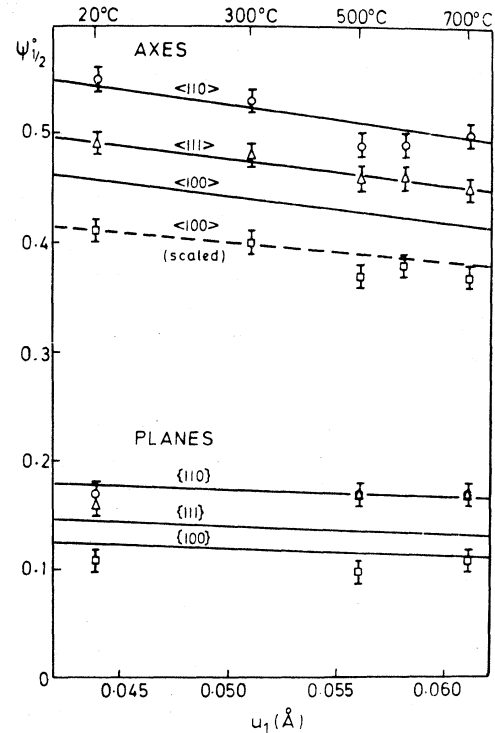


FIG. 7. Dependence of surface critical angles on thermal vibration amplitude. \circ for $\langle 110 \rangle$, $\{110\}$; Δ for $\langle 111 \rangle$, $\{111\}$; \square for $\langle 100 \rangle$, $\{100\}$; solid line is theory.

um model by assuming that a critical approach distance to the channel walls (atomic rows or planes, respectively) discriminates between channeled and nonchanneled ions, by putting this critical distance ρ_c equal to mu_1 , and by applying conservation of energy to the ion's transverse motion in order to obtain a critical approach angle ψ_c ; finally, $\psi_{1/2}$ is put equal to $k\psi_c$. Both k and m are proportionality constants of the order of unity. It is of interest that such an approach is evidently still appropriate in the case of diamond, in which $u_1 \ll a$, as was pointed out in I. It was originally suggested by Lindhard¹¹ that perhaps $\rho_c \sim a$ —with an implication that ρ_c would be determined by a (and that thermal vibrations would play the rôle of a perturbation). The former is usually valid (but only because $a \sim u_1$ for most substances), but the latter is not valid; the accuracy with which Eqs. (1) and (2) have been found to represent the functional dependence of $\psi_{1/2}$ on u_1 for many substances has led to the conclusion that ρ_c is in fact determined by u_1 . The results for diamond, in which $u_1 \approx 0.2a$, are clear and direct confirmation of this.

Varelas and Sizmann¹³ considered the proposal of Lindhard¹¹ and others that the continuum approximation was valid if the ion's "transverse kinetic energy" was sufficiently closely conserved. They per-

formed binary-collision calculations in order to investigate this fully under different conditions, and thereby to determine values of ρ_c and ψ_c for axial channeling. They were able to extend their calculations to rows with nonuniform interatomic spacing and mixed atomic species by the use of suitable combined parameters, obtaining slight differences from results using simple averages of d , Z_2 , etc. Their results are presented as universal functions of a reduced energy parameter in Ref. 13, together with a procedure for including the effect of thermal vibrations.

Some of the present diamond results are compared with their predictions in Table II. It is clear that $\psi_{1/2}$ should be compared, not with their ψ_c , but with $k\psi_c$, regarding the Barrett factor k as a generally applicable conversion factor between ψ_c and $\psi_{1/2}$. Agreement is excellent, with the exception once again of the $\langle 100 \rangle$ axis; Varelas and Sizmann's predictions agree with Barrett's (included in Table II) in all cases. It may be noted that $\langle 111 \rangle$ is an example of a string with nonuniform spacing.

The accuracy of Varelas and Sizmann's treatment seems to have been little appreciated hitherto. This may be because, in comparing their calculations with a large variety of experimental values, they compared their ψ_c with measured $\psi_{1/2}$ values,¹³ obtaining only fairly good agreement. Multiplying ψ_c by k produces much better agreement in most of these examples.

Morgan and van Vliet have published a series of papers¹⁴ in which the results of computer simulations of protons channeling in copper are expressed by analytic formulas. Their treatment of planes requires the use of an effective spacing \bar{d} which, for diamond, becomes negative for $E > 168$ keV. In the case of axes, too, their treatment seems to be rather far from its region of validity if applied to MeV ions in diamond.

Some workers^{15,16} have observed a stronger dependence of $\psi_{1/2}$ on u_1 than that predicted by Eq. (1), especially when $u_1/a \leq 0.8$. There is evidence for

this in Fig. 7 for the $\langle 110 \rangle$ and $\langle 100 \rangle$ axial data. The same may be true of $\langle 111 \rangle$; Varelas and Sizmann's treatment¹³ shows an inherent difference in the behavior of unequally spaced strings and predicts a slightly weaker temperature dependence for $\langle 111 \rangle$ than that plotted from Eq. (1), which used the mean interatomic spacing.

Mukherjee and Palmer¹⁶ devised a procedure for constructing row scattering potentials, after the form of the normal continuum potential, containing an extra proportion of the isolated atomic potential at distances closest to the row, and obtained good fits to their experimental temperature data for MgO. Instead of this, m in Eq. (1) could be allowed to vary. There is no *a priori* reason to assume that the relationship $\rho_c = mu_1$ should be linear; in fact, quadratic relationships have been used in other theoretical treatments.^{13,14} The diamond $\langle 110 \rangle$ and $\langle 100 \rangle$ data could be fitted by allowing m to increase from 1.2 at room temperature to 1.3(5) at 700°C, but the change was too small to determine the functional form of the relationship.

A few critical-angle measurements for channeling in diamond at room temperature have been reported by Picraux *et al.*,¹⁷ Sellschop and Gibson,¹⁸ and Braunstein *et al.*¹⁹ In Table III their values are compared with corresponding ones taken from the present work (where possible), and with theoretical values calculated by means of Eq. (1) or Eq. (2). There is reasonable agreement between the measurements of the different experimental groups, taking errors into account. The values found in the present experiments are generally slightly higher, and tend to agree more consistently with the theoretical estimates. This is in keeping with the larger experimental errors reported by the others.

In Figs. 2(a) to 2(f), it is noteworthy that all the curves in each family of channeling dips intersect at (or very close to) two common points, having a back-scattered yield $\chi \approx 80\%$. This was observed too in all

TABLE II. Critical angles ψ_c calculated by the method of Varelas and Sizmann (see text).

| Axis | E (MeV) | ρ_c (Å) | ψ_c (deg) | $k\psi_c$ (deg) | $\psi_{1/2}$ (deg) [Eq. (1)] | $\psi_{1/2}$ (expt) (deg) |
|-----------------------|-----------|--------------|----------------|-----------------|------------------------------|---------------------------|
| $\langle 110 \rangle$ | 1.0 | 0.065 | 0.66 | 0.55 | 0.54 | 0.55 |
| $\langle 111 \rangle$ | 0.6 | 0.075 | 0.74 | 0.62 | 0.63 | 0.62 |
| | 1.0 | 0.071 | 0.58 | 0.48 | 0.49 | 0.49 |
| | 2.5 | 0.066 | 0.38 | 0.31 | 0.31 | 0.30 |
| | 4.5 | 0.065 | 0.28 | 0.23 | 0.23 | 0.24 |
| $\langle 100 \rangle$ | 1.0 | 0.066 | 0.55 | 0.46 | 0.46 | 0.42 |

TABLE III. Comparison of diamond critical angles $\psi_{1/2}$ measured by different workers.

| Channel | Ion | E (MeV) | This work | Ref. 17 | $\psi_{1/2}$ (deg) | | Theory |
|---------|-----------------|-----------|-------------|-------------|---|-------------|--------|
| | | | | | Ref. 18 | Ref. 19 | |
| (110) | H ⁺ | 1.0 | 0.55 ± 0.01 | 0.54 ± 0.06 | 0.48 ± $\begin{smallmatrix} 0.02 \\ 0.01 \end{smallmatrix}$ | ... | 0.54 |
| | H ⁺ | 1.5 | ... | ... | 0.39 ± 0.02 | ... | 0.44 |
| | He ⁺ | 1.0 | 0.76 ± 0.02 | 0.75 ± 0.06 | ... | ... | 0.74 |
| (111) | He ⁺ | 2.0 | ... | ... | 0.53 ± 0.05 | ... | 0.52 |
| | H ⁺ | 0.35 | ... | ... | ... | 0.70 ± 0.05 | 0.83 |
| | H ⁺ | 1.0 | 0.49 ± 0.01 | 0.46 ± 0.06 | ... | ... | 0.49 |
| {110} | He ⁺ | 1.0 | 0.64 ± 0.01 | 0.58 ± 0.06 | ... | ... | 0.66 |
| | H ⁺ | 1.0 | 0.16 ± 0.01 | 0.16 ± 0.03 | ... | ... | 0.18 |

the measurements at other energies and with other ions. A speculative explanation is as follows. Trajectories with $\psi \approx \psi_{1/2}$ have a high dechanneling probability, whereas those with $\psi \approx 1.5\psi_{1/2}$, say, although mostly in the random beam,¹¹ have a high probability for "feeding in" to channels by multiple scattering. At some intermediate angle one might expect a balance between the two processes, and a constant yield with depth, the average ion spending about 80% of its time in the random beam.

It may further be noted that the "crossover angle" ψ_x was found to bear a constant relation to $\psi_{1/2}$. This is

$$\psi_{1/2} = \begin{cases} (0.84 \pm 0.02)\psi_x \\ (0.73 \pm 0.03)\psi_x \end{cases}$$

for axes and planes, respectively. These proportionality constants are remarkably similar to Barrett's values⁶ for k (0.83 for axes and 0.76 for planes) in Eqs. (1) and (2). It is tempting to speculate that the "critical angles" determined by these expressions, before application of the factor k , may be identified with ψ_x . In that case, ψ_x may represent the incidence angle of those trajectories which attain the critical approach distance ρ_c , with respect to the axis or plane in question.

The data of other workers were searched for the above phenomenon, replottting it if necessary. In some tungsten⁴ and gold²⁰ measurements, families of nested curves occur with no crossover; in PbS, the data¹⁵ are indistinct in the shoulder region; but for the tungsten curves of Anderson and Uggerhøj³ a crossover does appear to occur, with $\psi_{1/2} \approx 0.8\psi_x$. For zinc²⁰ (the only noncubic crystal for which data were available) a crossover is indicated with $\psi_{1/2}/\psi_x \approx 0.6$ or 0.9, depending on the axis. (All these measurements were for protons.) The effect should evidently be sought in other materials also.

IV. SUMMARY

We have presented a comprehensive set of consistent critical-angle data for the major axes and planes of diamond, and shown that the data are in most cases in agreement with accepted theoretical predictions. The two areas of disagreement contribute useful information: the fact that less close-packed axes require a smaller value of the proportionality constant in Eq. (1) confirms that inter-row focusing effects are important and depend on detailed crystal geometry; and the disagreement for unequally spaced planes both draws attention to the different nature of the channeling therein, and can be quantitatively interpreted in terms of the continuum model. There is some evidence for a stronger temperature dependence than simple theories require, and it has been suggested how this might be included. The remarkable invariance of the crossover points of the families of channeling dips for different depths of scattering was noted.

Diamond provides an extreme test of theory and of one's understanding of the channeling process. In particular, the importance of u_1 as the critical distance parameter is emphasized both in this work and in that reported in our previous paper (I) on minimum yields.

ACKNOWLEDGMENTS

We gratefully acknowledge the advice and assistance of the many past and present colleagues who helped bring this work to fruition; notably, Dr. D. W. Mingay for much advice and for his expertise with accelerators, the staff members of the mechanical and electronics workshops and the techniques laboratory for the construction of apparatus and for other

practical help, the successive generations of accelerator technicians for their efforts, the computer staff, and all those who helped collect data at night. We thank the University of the Witwatersrand, the de Beers Diamond Research Laboratory, the Chamber of Mines of South Africa, and the Council for Scientific and Industrial Research, for financial support.

APPENDIX: RECALCULATION OF {111} CRITICAL ANGLES

The arrangement of {111} planes in diamond is illustrated in Fig. 8. It is assumed that ions are confined to the wider interplanar gap (spacing d_2) with the critical angle governed by the distance of closest approach ρ_c to the two planes P_1 forming its walls; ρ_c is set equal to mu_1 , where u_1 is the rms thermal vibration amplitude and m is taken to have the same

value as for single planes ($= 1.6$). Then in calculating the critical angle ψ_c , by equating the initial transverse kinetic energy $E\psi_c$ to the change in potential energy between midchannel and ρ_c , the potentials due to all four planes (P_1 and P_2) are taken into account.

To avoid repetition, the treatment outlined by Gemmell⁷ for equally spaced planes, leading to his Eqs. (2.42) and (2.43), will be assumed. The result may be written in Gemmell's notation as

$$\psi_c = \psi_a (\Sigma f_{ps})^{1/2},$$

where the characteristic channeling angle is given by

$$\psi_a = (2\pi Z_1 Z_2 e^2 a N d_p / E)^{1/2},$$

and the sum is the result of summing the potentials of the two adjacent planes (and normalizing to zero at midchannel). For {111} planes, the sum is to be evaluated for both pairs of planes P_1 and P_2 , that is,

$$\psi_c = \psi_a \left[f_{ps} \left(\frac{\rho_c}{a} \right) + f_{ps} \left(\frac{d_2 - \rho_c}{a} \right) - 2f_{ps} \left(\frac{d_2}{2a} \right) + f_{ps} \left(\frac{\rho_c + d_1}{a} \right) + f_{ps} \left(\frac{d_1 + d_2 + \rho_c}{a} \right) - 2f_{ps} \left(\frac{2d_1 + d_2}{2a} \right) \right]^{1/2} = \psi_a F_{ps}^{(4)},$$

where, in Gemmell's notation,

$$F_{ps}^{(4)} = \left\{ \left[F_{ps} \left(\frac{\rho_c}{a}, \frac{d_2}{a} \right) \right]^2 + \left[F_{ps} \left(\frac{\rho_c + d_1}{a}, \frac{2d_1 + d_2}{a} \right) \right]^2 \right\}^{1/2} = \{ [F_{ps}(\xi, \eta)]^2 + [F_{ps}(\xi', \eta')]^2 \}^{1/2}$$

with

$$\begin{aligned} \xi &= \frac{\rho_c}{a}, \\ \eta &= \frac{d_2}{a}, \\ \xi' &= \frac{\rho_c + d_1}{a}, \\ \eta' &= \frac{2d_1 + d_2}{a}. \end{aligned}$$

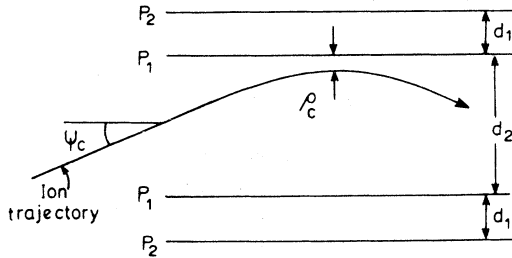


FIG. 8. Model of {111} planar channeling in the diamond lattice, as developed in the appendix. The spacings are $d_1 = 0.515 \text{ \AA}$; $d_2 = 1.545 \text{ \AA}$.

The values of $F_{ps}(\xi, \eta)$ and $F_{ps}(\xi', \eta')$ were evaluated from the curves in Ref. 7, giving

$$F_{ps}^{(4)} = 0.92.$$

Then, by analogy with Eq. (2),

$$\psi_{1/2} = k F_{ps}^{(4)} \psi_a, \quad (3)$$

where the value of d_p to be used in calculating ψ_a is the mean value, since d_p enters the expression via the atomic density in the plane, which is determined by the mean planar spacing. The resulting values of

TABLE IV. Recalculated values of {111} planar critical angles.

| E (MeV) | $\psi_{1/2}$ (deg) [Eq. (3)] | $\psi_{1/2}$ (expt) (deg) |
|-----------|------------------------------|---------------------------|
| 0.6 | 0.25 | 0.24 |
| 1.0 | 0.19 | 0.17 |
| 2.5 | 0.12 | 0.11 |
| 4.5 | 0.09 | 0.08 |

$\psi_{1/2}\{111\}$ for protons are compared with the experimental ones in Table IV. The agreement is good, indicating the validity of the model of $\{111\}$ channeling used.

It has been suggested^{7,21} that two distinct channeling components ought to be observable, with dif-

ferent critical angles corresponding to the two interplanar spacings. There was no sign of this in the diamond measurements, in the form of inflections in the sides of the channeling dip; any ions initially so channeled must be rapidly dechanneled into the wider spaces or into the random beam.

-
- ¹T. E. Derry, R. W. Fearick, and J. P. F. Sellschop, *Phys. Rev. B* **24**, 3675 (1981).
- ²J. H. Barrett, *Phys. Rev.* **166**, 219 (1968).
- ³J. U. Andersen and E. Uggerhøj, *Can. J. Phys.* **46**, 517 (1968).
- ⁴For example, see J. A. Davies, J. Denhartog, and J. L. Whitton, *Phys. Rev.* **165**, 345 (1968).
- ⁵M. A. Kumakhov, V. A. Muralev, A. S. Rudnev, and E. I. Sirotin, *Radiat. Eff.* **24**, 273 (1975).
- ⁶J. H. Barrett, *Phys. Rev. B* **3**, 1527 (1971).
- ⁷D. S. Gemmell, *Rev. Mod. Phys.* **46**, 129 (1974).
- ⁸A. C. Victor, *J. Chem. Phys.* **36**, 1903 (1962).
- ⁹J. H. Barrett, *Phys. Rev. Lett.* **31**, 1542 (1973).
- ¹⁰J. Lindhard, *Phys. Lett.* **12**, 126 (1964).
- ¹¹J. Lindhard, *K. Dan. Vidensk. Selsk. Mat.-Fys. Medd.* **34**, No. 14 (1965).
- ¹²J. U. Andersen and L. C. Feldman, *Phys. Rev. B* **1**, 2063 (1970).
- ¹³C. Varelas and R. Sizmann, *Radiat. Eff.* **16**, 211 (1972).
- ¹⁴D. V. Morgan and D. van Vliet, *Radiat. Eff.* **8**, 51 (1971), and references therein.
- ¹⁵J. U. Andersen and E. Laegsgård, *Radiat. Eff.* **12**, 3 (1972).
- ¹⁶S. D. Mukherjee and D. W. Palmer, *Phys. Lett.* **74A**, 97 (1979).
- ¹⁷S. T. Picraux, J. A. Davies, L. Eriksson, N. G. E. Johansson, and J. W. Mayer, *Phys. Rev.* **180**, 873 (1969).
- ¹⁸J. P. F. Sellschop and W. M. Gibson, *Diamond Research, 1973* (Industrial Diamond Information Bureau, London, 1973), p. 32.
- ¹⁹G. Braunstein, A. Talmi, R. Kalish, T. Bernstein, and R. Beserman, *Radiat. Eff.* **48**, 139 (1980).
- ²⁰L. M. Howe and S. Schmid, *Can. J. Phys.* **49**, 2321 (1971).
- ²¹B. R. Appleton, L. C. Feldman, and W. L. Brown, Brookhaven National Laboratory Report No. BNL-50083 (unpublished), p. 45.